



## **Flight Qualification of the Red Kite Solid Rocket Motor**

*T. Röhr<sup>1</sup>, F. Scheuerpflug<sup>1</sup>, J. Ettl<sup>1</sup>, D. Kail<sup>1</sup>, C. Mildenberger<sup>1</sup>, J. Riehmer<sup>2</sup>, C. Schnepf<sup>3</sup>, R. Kirchhartz<sup>1</sup>*

### **Abstract**

The Red Kite<sup>®</sup> is a commercially available, serially produced solid propellant sounding rocket motor in the class of one ton of net explosive mass. It was flight qualified in November 2023 at the Andøya Space launch site in Norway after four years of development. The flight was named SOAR (*Single Stage Operational Assessment of Red Kite*) and was administered by DLR Mobile Rocket Base. Main objective of the flight was to collect a body of data sufficient to validate flight worthiness of the Red Kite. Secondary objective was to propel APEX-TD (*Air Breathing Propulsion Experiment - Technology Demonstrator*) by the DLR Institute of Aerodynamics and Flow Technology to high speed in the low atmosphere to enable in-situ research on the air flow inside a scramjet type duct. Both objectives required live streaming of data to ground because the vehicle was not equipped with a parachute recovery system. Both objectives were fully met. The vehicle reached an apogee of 71 km, a maximum speed of Mach 4.8 and impacted in the Norwegian Sea 58 km from the launch site. Key trajectory parameters are all within one standard deviation of predictions. Thus, SOAR demonstrated the capability of Red Kite and DLR MORABA supplementary systems to provide the scientific community with an easy, reliable and highly customizable flight from one of multiple launch sites around the world. The paper describes the SOAR objectives, design, execution and results including noteworthy observations from vehicle and ground based instruments.

**Keywords:** *Solid Rocket Motor, Flight Platform, Flight Testing, In-Situ Research, Mission Design*

### **1. Objectives**

Main objective of project SOAR (*Single Stage Operational Assessment of Red Kite*) was to flight qualify the Red Kite solid propellant rocket motor developed in cooperation between DLR MORABA and Bayern-Chemie GmbH from 2020 to 2023. Red Kite had already been tested successfully in two static firings in August 2023 at Esrange, Sweden. The role of flight testing was to confirm that Red Kite would perform nominally under the additional inertial and aerodynamic loads and to rule out excessive thrust misalignment. Further, compatibility of Red Kite with existing systems (radar, telemetry, launcher, on-board data acquisition), handling and operations were tested in the field. For the complete development history and the application spectrum of the Red Kite motor refer to [1].

The secondary objective was to establish suitable flow conditions for APEX-TD (*Air Breathing Propulsion Experiment - Technology Demonstrator*). This required to fly fast in the low atmosphere and to actively open the inlet of the scramjet type duct shortly after motor burn-out. The relevant altitude band was < 40 km, both ascent and descent were of interest. The results of APEX-TD are not discussed in this paper, the interested reader is referred to [2].

---

<sup>1</sup> DLR, Institute of Space Operations and Astronaut Training – Department Mobile Rocket Base, Münchener Straße 20, 82234 Weßling, Germany, [Thomas.Roehr@DLR.de](mailto:Thomas.Roehr@DLR.de), [Frank.Scheuerpflug@DLR.de](mailto:Frank.Scheuerpflug@DLR.de), [Josef.Ettl@DLR.de](mailto:Josef.Ettl@DLR.de), [Dietmar.Kail@DLR.de](mailto:Dietmar.Kail@DLR.de), [Christian.Mildenberger@DLR.de](mailto:Christian.Mildenberger@DLR.de), [Rainer.Kirchhartz@DLR.de](mailto:Rainer.Kirchhartz@DLR.de)

<sup>2</sup> DLR, Institute of Aerodynamics and Flow Technology – Department Supersonic and Hypersonic Technologies, Linder Hoehe, 51147 Cologne, Germany, [Johannes.Riehmer@DLR.de](mailto:Johannes.Riehmer@DLR.de)

<sup>3</sup> DLR, Institute of Aerodynamics and Flow Technology – Department High Speed Configurations, Bunsenstr. 10, 37073 Göttingen, Germany, [Christian.Schnepf@DLR.de](mailto:Christian.Schnepf@DLR.de)

## 2. Design

In the design of SOAR, simplicity was key to meet the tight project schedule and minimize cost and development risk. This meant to fly single stage, with no active guidance, with no active spin-up or despin maneuvers and no attitude or rate control systems. No objects were separated from the vehicle during flight allowing for reliable radar skin track without a transponder.

### 2.1. Vehicle

The vehicle measured 6.6 m in length and 0.56 m (22") in motor diameter. Lift-off mass was 1570 kg of which approximately 900 kg were solid propellant and 250 kg payload mass. It is shown in Fig 1.

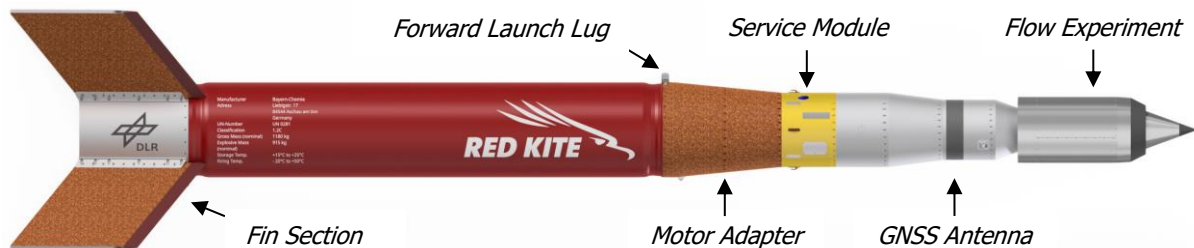


**Fig 1.** SOAR vehicle

Hardware compatibility was a major design driver in the development of Red Kite. Fin section and motor adapter have flight heritage from the VSB-30 sounding rocket and can be swapped between Red Kite and VSB-30 without adjustments. The 17" diameter service module had been flown multiple times in the MAPHEUS program, it was refurbished and upgraded for SOAR. Typically, for spinning vehicles, the global navigation satellite system (GNSS) antenna is mounted at the very tip of the vehicle. This was not possible since the flow experiment had a custom, instrumented nose-tip. Thus, a GNSS wrap-around antenna was mounted in the 14" diameter section of the payload.

The four fins are of aluminum sandwich construction with a simple rhomboid planform, a phenolic composite leading edge and a cork thermal protection layer. They were canted at  $0.4^\circ$  to produce about 2 Hz of positive spin for decreased impact point dispersion.

### 2.2. Interfaces

The SOAR vehicle interfaced the launch rail via two T-shaped launch lugs. They were released simultaneously after 16 m of rail travel to avoid 'tip-off' which is a type of vehicle-launcher interaction. Prior to launch, power supply and communications to the vehicle were established via the service module interface rack mounted on the launcher beam. The interface rack connects to the vehicle via a single RS-422 umbilical hardline and to the range network via ethernet. In the control room, a new ground support concept was rolled out that uses a virtualization cluster with virtual machines for computing and allows for faster deployment of mission specific configurations. The vehicle was ignited via a six-pole firing line transmitting ARM signal, FIRE signal and a feedback loop. The ARM signal was provided by the Red Kite Arming Console, the FIRE signal was provided by the launch range.

### 2.3. Instrumentation

Instrumentation focused on these measurands that were deemed essential for flight qualification:

- trajectory, motor pressure and acceleration as indicators of motor performance;
- vehicle attitude as an indicator of thrust misalignment or aerodynamic defects.

The trajectory was measured on-board by one Phoenix GNSS receiver and from ground by telemetry slant range and by radar skin track. To improve slant range measurements the service module carried a chip-scale atomic clock oscillator. Accelerations and rates were measured by two dissimilar inertial measurement units (IMU), integration of IMU data provides the vehicle attitude as well as another source of trajectory information. The motor pressure was measured on-board by two dissimilar pressure sensors sampled by independent data acquisition systems and send to ground by independent transmitters. Other on-board instrumentation included temperature and vibration sensors as wells as optical cameras. The S-band telemetry streams were received by Andøya Space with both a 6 m and a 3 m antenna.

## 2.4. Aerodynamics

The majority of the aerodynamic dataset has been determined with the DLR-TAU Code. The remainder was calculated with semi-empirical tools.

TAU is a hybrid structured / unstructured finite volume flow solver based on the compressible Reynolds-Averaged Navier-Stokes equations. For the current study steady simulations with a second-order upwind spatial discretization scheme have been performed. The Spalart-Allmaras one-equation turbulence-model was used to close the system of equations. For comparison, also Menter's shear stress transport model was applied. A fully turbulent boundary layer was assumed for all altitudes and Mach numbers investigated. Simulations have been performed for the open, closed and intermediate state of the hypersonic experiment with a computational mesh size of about 60 million degrees of freedom. Fig 2 shows the flow and shock systems at Mach 5.15 for illustration.

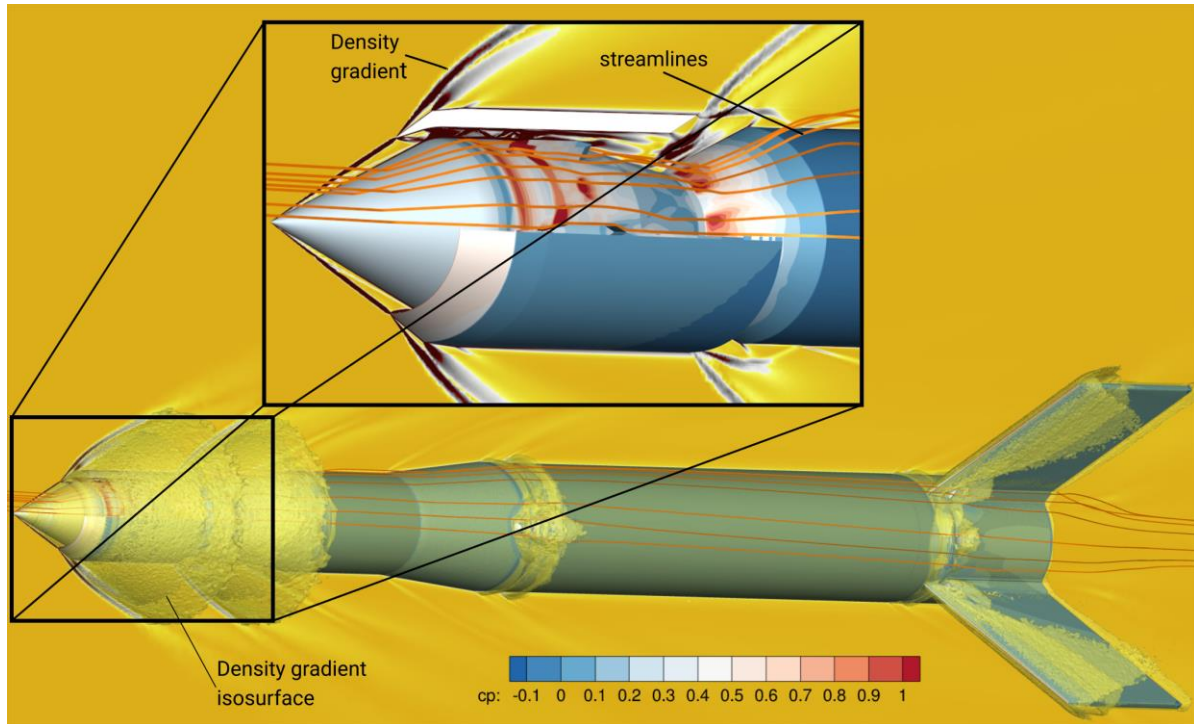


**Fig 2.** Exemplary flow state, Mach 5.15, 10 km altitude, 1° angle of attack

One important constraint of aerodynamic design is static margin, the distance between the center of gravity and the static center of pressure. For a typical sounding rocket mission with a proven vehicle the static margin requirement would be  $\geq 1.5$  motor diameter ('caliber'). For SOAR the requirement was increased to  $\geq 2.0$  caliber considering added uncertainty from the complexity of the internal flow path through the forebody. The APEX-TD forebody design was iterated to comply with this requirement as described in [2]. Fig 3 gives the final static margin prediction showing that the internal flow path reduces static margin by 0.4 caliber.

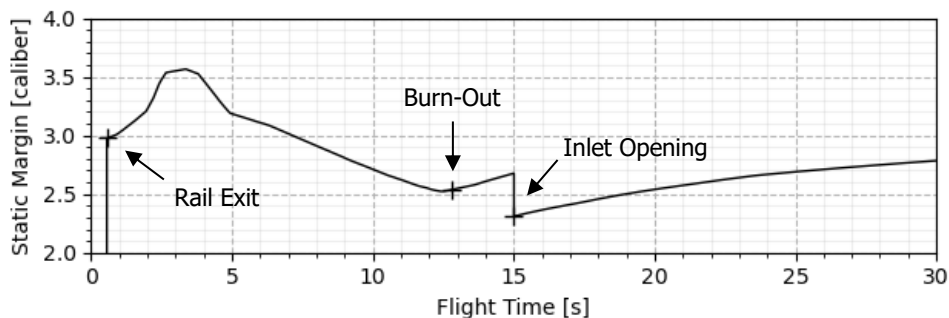


**Fig 3.** Static margin prediction during early flight

### 3. Execution

#### 3.1. Schedule

Major milestones of the SOAR project are given in Table 1:

**Table 1.** Project milestones

<b>Kick-Off Meeting</b>	<b>Avionics Testing Week</b>	<b>Environmental Testing Week</b>	<b>Equipment Transport</b>	<b>Launch</b>
January 12th	October 9th	October 16th	October 30th	November 13th

#### 3.2. Avionics testing

Avionics testing was conducted at the DLR Oberpfaffenhofen site in Germany. It included multiple communication checks between all flight systems, functional tests of the APEX-TD payload events as well as all-up flight simulation runs with telemetry and simulated lift-off. The payload events, namely pneumatic opening of the inlet at T+15 s and inert gas injection into the internal flow path between T+20 s and T+80 s, were commanded by the service module according to a pre-programmed timeline.

#### 3.3. Environmental testing

Environmental testing was done at the facilities of Airbus Defence and Space and of iABG, both in Ottobrunn, Germany. The 'forward stack' comprising every module forward of the rocket motor was measured for length, mass, center of gravity (CG) and mass moment of inertia. It was spin balanced at 2 Hz until static and dynamic imbalance and tip runout met the flight dynamics requirements. The values achieved were 0.015 kg\*m, 0.006 kg\*m<sup>2</sup> and 0.8 mm, respectively. Fig 4 shows the forward stack during CG measurement at Airbus. In the background on the right-hand side is one of the two shaker tables used for vibration testing.

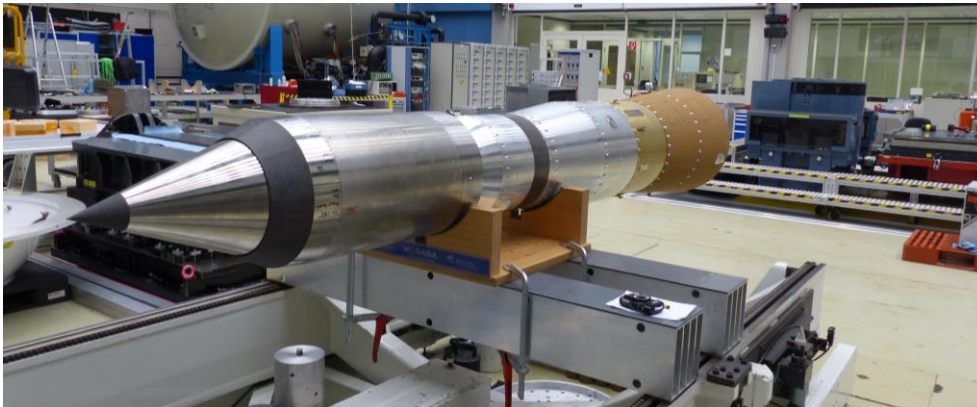


**Fig 4.** Forward stack during CG measurement

The forward stack was vibration tested in roll, pitch and yaw axis using a random vibration spectrum in the 20 – 2000 Hz range with 12.7 g root-mean-square (grms) acceleration. This spectrum was adopted from [3] because in-flight vibration data for the Red Kite motor was not yet available. The 2 – 3 grms level measured during static firing at the axial load adapter [1] was deemed overly optimistic when considering the fixation of the motor to the test bench. Halfway through each 30 s random vibration run the APEX-TD inlet was opened pneumatically to demonstrate this feature under load.

#### 3.4. Flight campaign

The flight campaign was conducted at the Andøya Space launch site in Norway, November 7<sup>th</sup> to 16<sup>th</sup> 2023. Contrary to many other sounding rocket motors, Red Kite is shipped with nozzle-extension, igniter and initiator installed. This resulted in a short preparation time of three days for the motor section. Preparations included income inspection, fin-section installation, fin cant angle adjustment, and motor pressure sensor calibration and installation. Meanwhile, the forward stack was assembled and tested in the payload assembly building. Another series of all-up flight simulations was conducted, this time including range infrastructure such as the telemetry station into the test. The forward stack was joined with the motor horizontally on day 5. The vehicle was loaded to the U3 launcher, the umbilical

hardline was connected, and the service module was clad in Styrofoam for thermal insulation. Remote controlled support arms were used to support the payload weight prior to launch, thus taking the bending load off the motor front joint. Fig 5 illustrates the process.



**Fig 5.** (a) motor as delivered, (b) vehicle fully assembled, (c) during loading, (d) during countdown

On November 13<sup>th</sup>, after a test countdown in the morning, it was decided to go for a hot countdown the same day as weather forecasts predicted a steep increase in cloud coverage, precipitation and wind speeds for the following days. SOAR was launched on November 13<sup>th</sup> 2023, 12:20:00 UTC, at 78.3° elevation, 324.1° azimuth, to a perfectly blue sky and low wind speeds.

Fig 6 shows SOAR travelling along the launch rail, debris in the exhaust stems from the Styrofoam cladding. Analysis of high-speed video footage indicates nominal umbilical release. The on-board video was live-streamed and is available at [4].



**Fig 6.** Lift-off from the U3 launcher at Andøya Space

## 4. Results

Motor data and experiment data were sent and received continuously from lift-off until shortly before impact. Loss of signal was at 12:24:17 UTC, at 69.75653° geodetic latitude, 15.32192° longitude and 235 m altitude according to GNSS. Flight data was compared with simulations to confirm nominal performance. Several simulations were conducted incorporating data measured during the flight in an effort to reconstruct the actual trajectory as closely as possible. This process of reconstruction can give valuable insight into which factor might have caused an observed deviation.

Table 2 gives an overview of the simulation inputs. T-zero wind is the wind profile at lift-off from ground up to 28 km altitude compounded from balloon soundings and wind tower anemometers. Calibrated thrust is the nominal thrust time history multiplied by a time-dependent calibration factor based on comparison of nominal and in-flight measured motor pressure. Air density is taken from the 1962 International Standard Atmosphere (ISA62) and from a balloon launched at T-28 minutes. Best Match is a simulation optimized for apogee and impact coordinate match obtained by appropriate adjustment of launcher settings and overall drag coefficient.

**Table 2.** Simulation inputs

<b>Name:</b>	<b>Nominal</b>	<b>T-Zero</b>	<b>Calibrated</b>	<b>Best Match</b>
Launcher settings:	Nominal: 80.0° elevation, 330.0° azimuth	T-zero: 78.3° elevation, 324.1° azimuth	T-zero: 78.3° elevation, 324.1° azimuth	Best match: 78.5° elevation, 324.5° azimuth
Thrust model:	Nominal	Nominal	Calibrated	Calibrated
Air density model:	ISA62	ISA62	<28 km: balloon >28 km: ISA62	<28 km: balloon >28 km: ISA62
Drag model:	Nominal	Nominal	Nominal	Best match
Wind model:	No wind	T-zero	T-zero	T-zero

### 4.1. Flight trajectory

Fig 7 and Fig 8 show excellent agreement of GNSS and radar track with spatial distance below 100 m throughout the trajectory (except for one notable exception discussed later). Integration of IMU data from the service module (SM) yields a trajectory that agrees well for most of the flight. At 10 km descent altitude, the SM IMU track starts to diverge as integration errors accumulate which is a common observation for missions with highly dynamic reentry.

According to GNSS, apogee is 71.2 km (nominal: 75.2 km), impact ground range is 58.4 km (nominal: 60.5 km). Compared to pre-flight dispersion estimates, both apogee and impact point are within one standard deviation ( $1 \sigma$ ). The 1, 2 and 3  $\sigma$  dispersion ellipses are visualized in Fig 7, they represent bivariate normal distributions, probability of impact within 1, 2 and 3  $\sigma$  is 39.4%, 86.5% and 98.9%, respectively.

When including the T-zero wind profile and the final launchers settings into the 'T-Zero' simulation, the match with flight data gets slightly worse in terms of ground range but better in terms of heading as shown in Fig 8. The best match with GNSS and radar track is achieved by assuming 0.2° higher launcher elevation, 0.4° higher launcher azimuth and a 5% higher overall vehicle drag coefficient. As an alternative to 5% higher drag, a 30 kg higher lift-off mass may be assumed with similar results. Realistically, the observed flight path deviation is the result of a combination of factors.

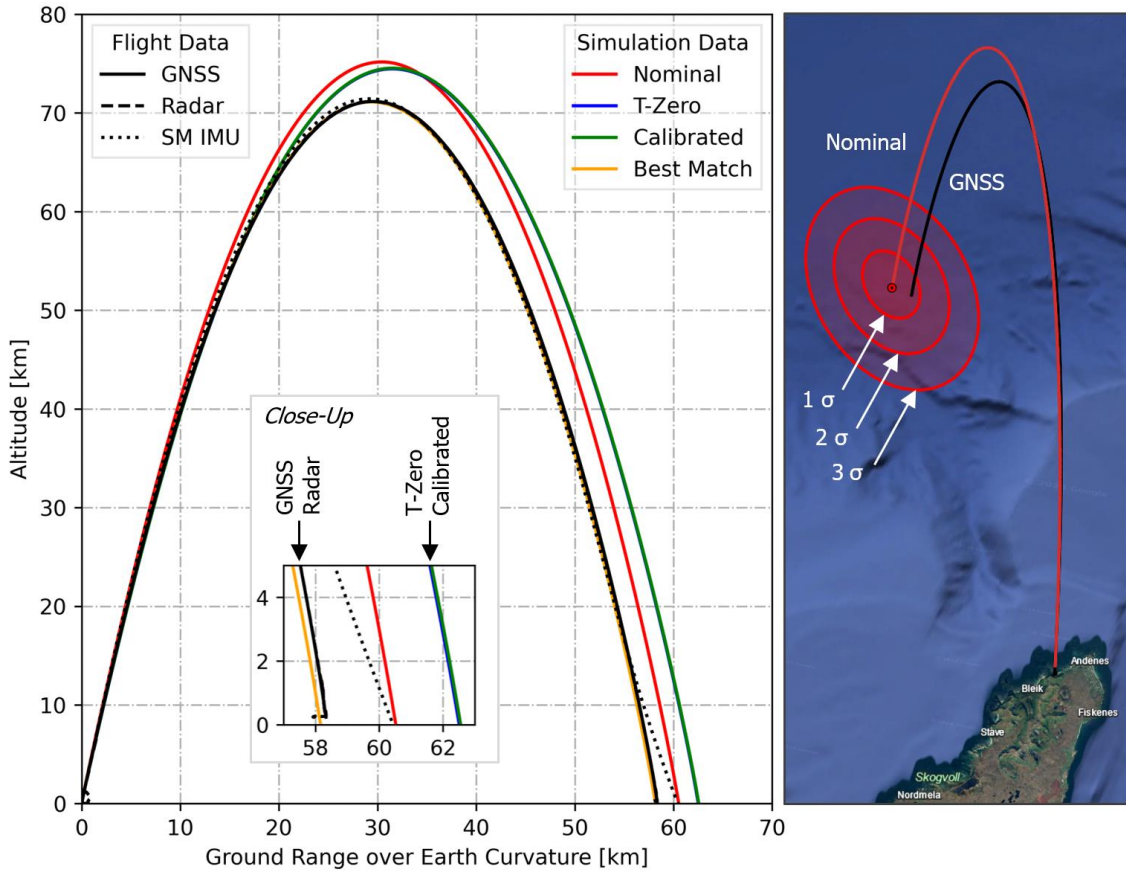


**Fig 7.** Altitude over ground range and predicted dispersion

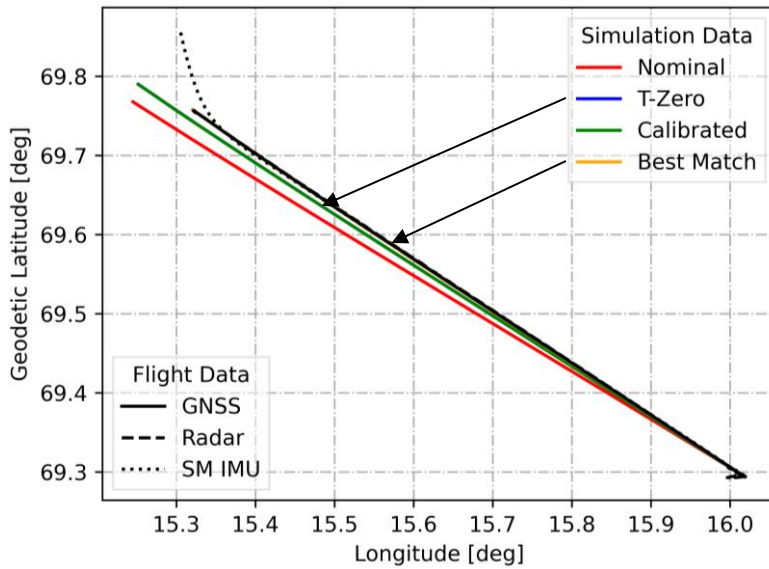


**Fig 8.** Ground track

The two motor pressure measurements agree well between T+2 s and T+12 s. The data was compared with the nominal motor pressure profile. The time-dependent delta was then used to calibrate the nominal thrust profile. The result is presented in the upper half of Fig 9. The calibrated thrust profile (green curve) is slightly higher during the boost phase and the transient phase of the dual-thrust profile but slightly lower during the sustainer phase.

The calibrated thrust profile yields an improved match with acceleration data from the service module IMU as shown in the bottom half of Fig 9. This suggests that the thrust profile was, indeed, slightly more aggressive than predicted. That being said, the amount of variation seen here is considered fully

acceptable for the sounding rocket application. The essential parameter for trajectory prediction, total impulse, is very similar as demonstrated by the identical apogee of 'T-Zero' and 'Calibrated' shown in Fig 7. To be exact, another simulation parameter, namely atmospheric density, was also adjusted between 'T-Zero' and 'Calibrated', however, with little effect on any of the data presented here.

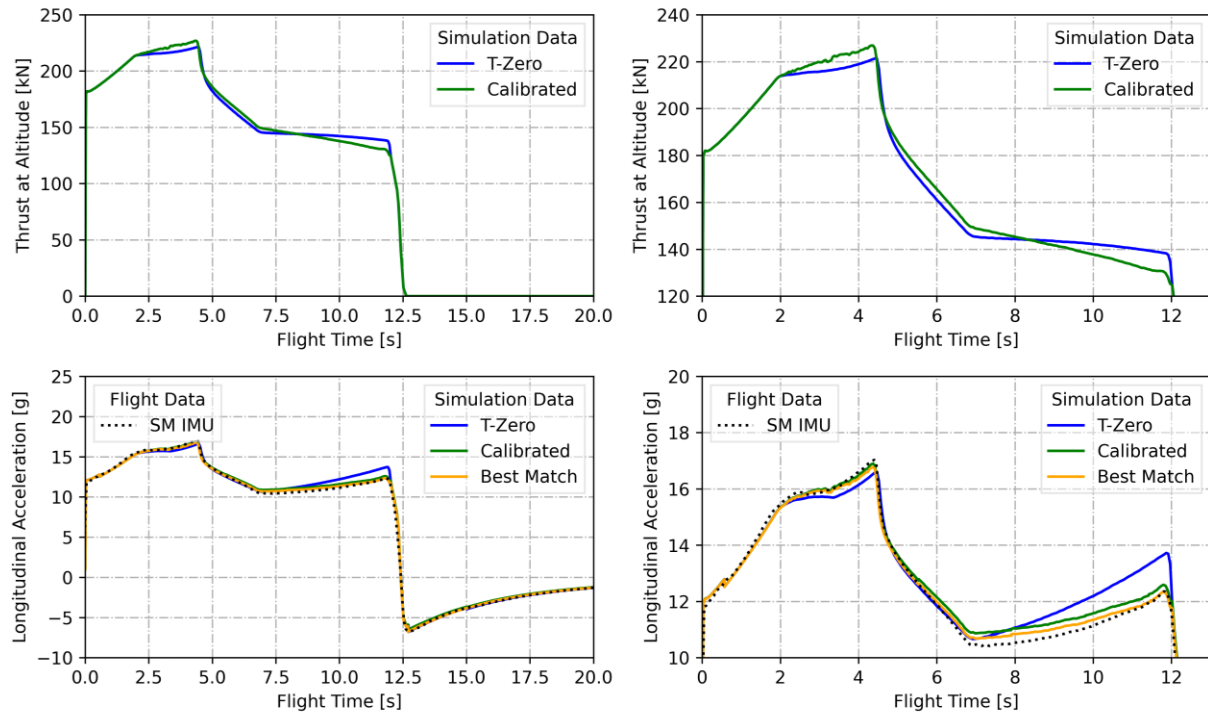


**Fig 9.** Thrust input and resulting acceleration versus flight data

Finally, Fig 10 gives flight speed and local Mach number. Except for a small artifact at T+1.5 s the GNSS data is unremarkable. The maximum flight speed of 1425 m/s matches well with simulations, the maximum Mach number is 4.8. Speed of sound is based on temperature data from a balloon sounding at T-28 minutes. Maximum dynamic pressure was experienced upon motor burn-out at 10 km altitude, it was 473 kPa according to the best match simulation.

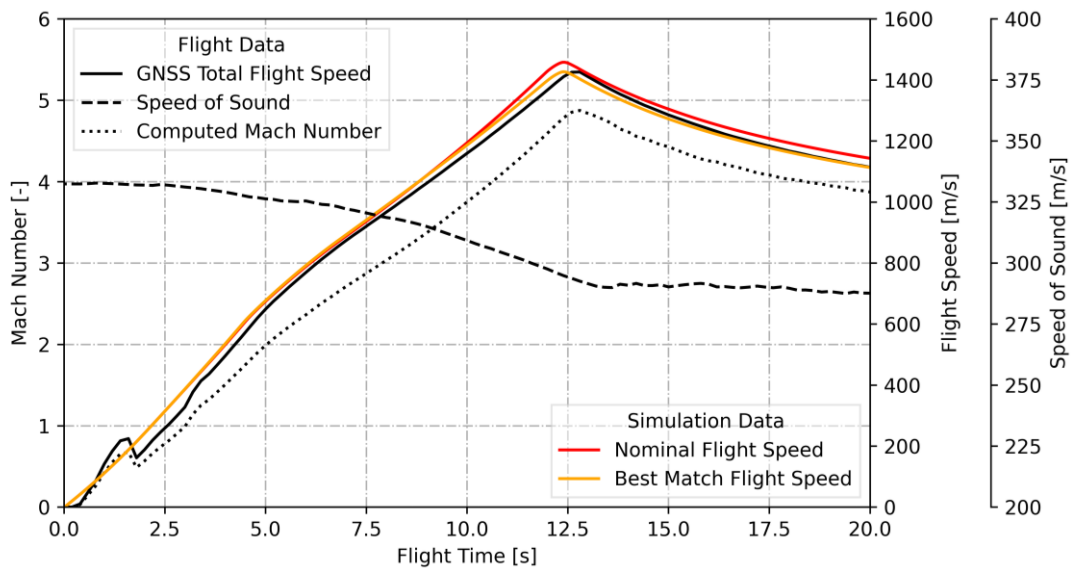
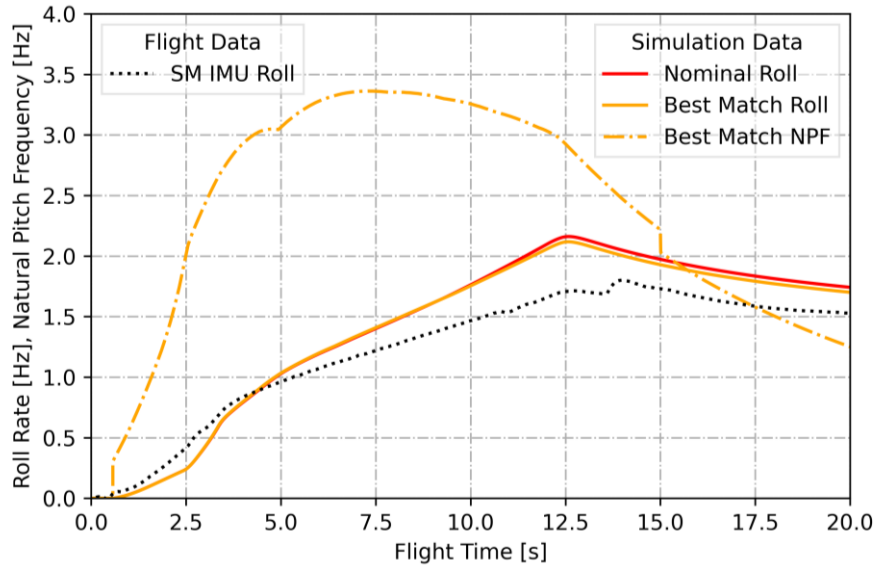


**Fig 10.** Total flight speed and Mach number



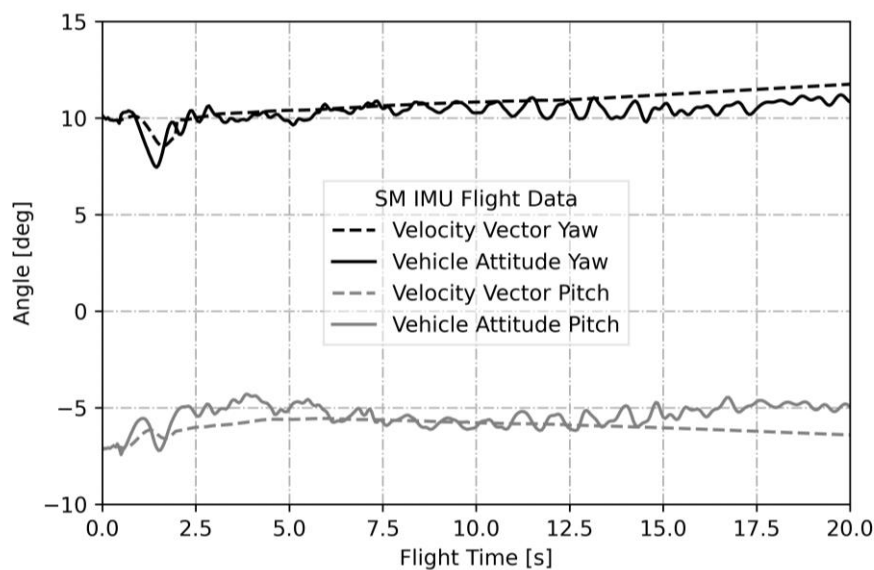
### 4.2. Roll and attitude

Fig 11 gives the roll build-up demonstrating reasonable agreement of predictions and flight data. The maximum roll rate is 1.80 Hz which is 0.36 Hz short of nominal. The data suggests an overestimation of the roll-driving coefficient in the supersonic regime. This is not completely surprising considering that roll-driving and roll-damping were not produced with DLR-TAU Code but with lesser fidelity semi-empirical tools. Measured roll rate and best match natural pitch frequency (NPF) cross at T+17.5 s. Investigating vehicle roll rate and attitude around this so-called 'pitch-roll-crossing' can be particularly instructive since anomalous flight behavior may be amplified, but no such amplification was found.



**Fig 11.** Roll build-up and natural pitch frequency

Fig 12 gives the attitude of the velocity vector or flight path and the attitude of the vehicle roll-axis in the local frame. The local frame is vehicle carried with pitch pointing north, yaw pointing west and the third axis pointing up as normal on the WGS84 ellipsoid. Naturally, the vehicle attitude oscillates around the velocity vector. The amplitude is small, approximately 1° peak-to-peak, and steady over burn phase and coast phase suggesting that there was little, if any, thrust misalignment. Thrust misalignment can be caused for example by manufacturing tolerances or uneven burning and is a major concern when launching an unguided sounding rocket as it drives impact point dispersion.



**Fig 12.** Velocity vector and vehicle attitude

### 4.3. Vibration

Vibration was measured in the motor adapter near the skin by a triaxial piezo electric accelerometer. The measurement was intended to be the basis of a vibration envelope that could be handed out to customers for payload qualification and acceptance testing. Data was received but is deemed implausible. Temporary over-loading of the accelerometer was identified as the most likely reason. DLR plans to repeat the vibration measurement as soon as possible using a sensor with higher load rating.

### 4.4. Radar track during motor burn

The DLR mobile range instrumentation radar RIR-774-C at Lidar Bygg (69.295519° N, 16.033552° E) skin tracked the vehicle for most of the flight with great accuracy. Only during the first 10.2 s (up to 1.5 km ground range) does the radar track deviate visibly from GNSS as shown in Fig 13. Automatic gain control (AGC) recordings indicate a large amount of 'clutter' reflections that make identification of the vehicle echo difficult. Despite this, the radar operators were able to acquire and track the vehicle manually. At T+10.2 s, the vehicle echo was clearly distinguishable, so the operators switched to automatic tracking mode. Fig 14 gives two stills from the AGC recording for illustration.

According to one hypothesis, the clutter is caused by metal particle content in the motor exhaust plume that creates additional reflections while dampening the vehicle echo. This is supported by the fact that the effect is only observed during the motor burn phase. Another potential source of clutter is heavy clouds or rain, but neither was present at time of launch.

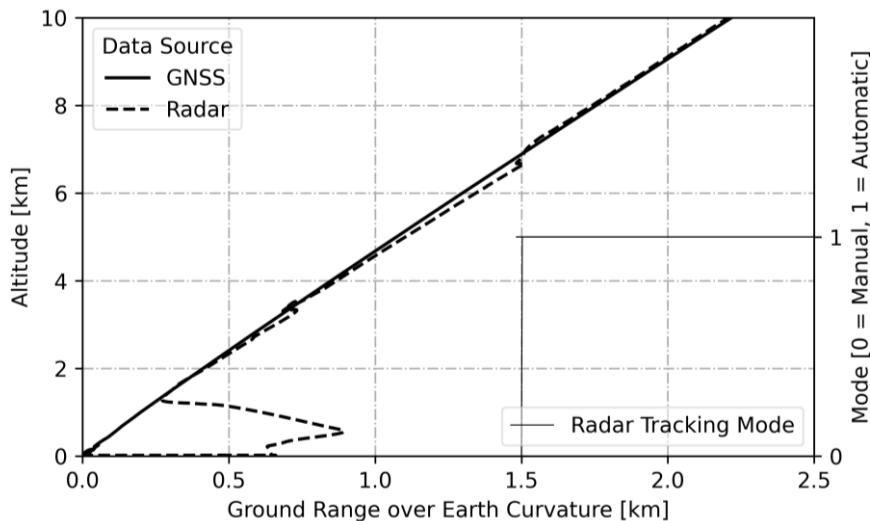


**Fig 13.** Radar versus GNSS track during motor burn

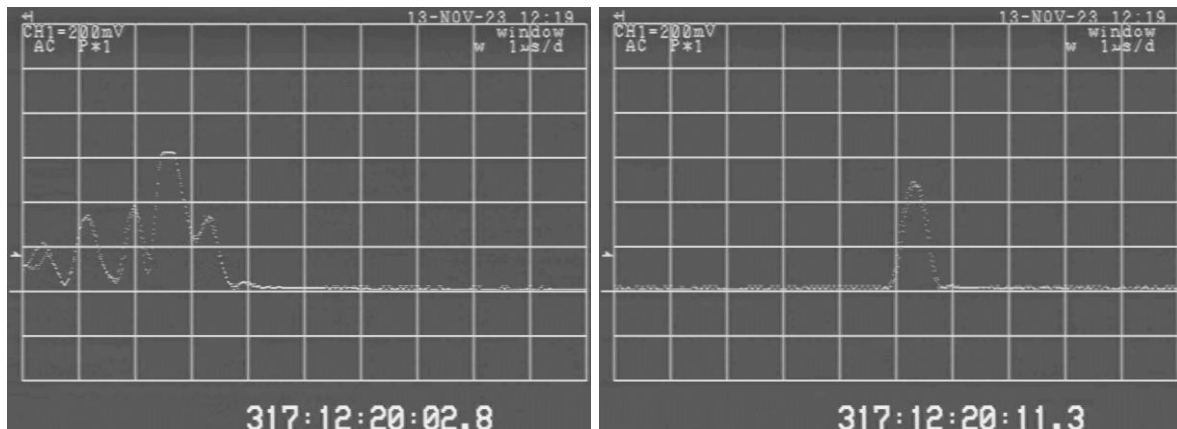


**Fig 14.** RIR-774C AGC recording at T+2.8 s (left) and T+11.3 s (right)

## 5. Summary

Data acquisition, transmission and reception were on the whole very successful resulting in a large body of data available for post-flight analysis. Key trajectory parameters are all within one standard deviation of predictions. The deviations could, to date, not be attributed to any single source. Post-flight simulations suggest that the motor thrust profile is accurate. Atmospheric density was also ruled out as a major contributor. The best match of simulated and observed trajectory is achieved when assuming slightly altered launcher settings ( $+0.2^\circ$  elevation,  $+0.4^\circ$  azimuth) and 5% higher than modelled drag coefficient of the vehicle. Peak roll rate was about 20% lower than predicted, likely due to overestimation of the roll-driving coefficient. The vehicle attitude time history is unremarkable, there is no indication of any significant thrust misalignment or aerodynamic defects. Radar skin track was challenging during the motor burn phase which might be due to metal particles in the exhaust.

In all, the first flight of the Red Kite solid rocket motors was positively uneventful demonstrating the motors performance, quality and ease of handling in the field.

## 6. Outlook

Based on the positive results of flight qualification, the first regular flight of a Red Kite motor was conducted three months later on February 27<sup>th</sup> 2024. Combined with an Improved Malemute upper stage motor, Red Kite delivered a 440 kg microgravity payload to an apogee of 265 km in the 14<sup>th</sup> edition of the DLR MAPHEUS research program.

The authors are looking forward to see Red Kite employed in a variety of motor combinations in the coming years. ATHEAT scheduled for June 2025 is awaited with particular excitement as it aims to combine Red Kite with a Black Brant Mk4 sustainer motor to propel some 200 kg of payload to flight speeds above Mach 9 on a suppressed trajectory. The Red Kite application spectrum is described in detail in [1].

## 7. Acknowledgements

The authors want to express their gratitude towards DLR PK-S (Programmkoordination Sicherheit) for their financial support enabling the integration of the APEX-TD experiment into the qualification flight, thereby adding to the technical output of this project a great amount of valuable scientific data [2].

## References

1. Scheuerpflug, F., Röhr, T., Huber, T., Reinold, M., Hergarten, D., Kobow, L., Kirchhartz, R., Kuhn, M., Weigand, A., Berndl, M., Werneth, J.: The Red Kite Sounding Rocket Motor Qualification Milestones and Application Spectrum. 3rd HiSST, 14 – 19 April 2024, Busan
2. Riehmer, J., Klingenberg, F., Röhr, T., Schnepf, C., Zuber, C., Gülhan, A.: Design and Objectives of the Air-breathing Propulsion Experiment Technology Demonstrator (APEX-TD). 3rd HiSST, 14 – 19 April 2024, Busan
3. Burth, R.H., Cathell, P.G., Edwards, D.B., Ghalib, A.H., Gsell, J.C., Hales, H.C., Haugh, H.C., Tibbetts, B.R.: NASA Sounding Rockets User Handbook, Technical Publication 20230006855. <https://sites.wff.nasa.gov/code810/files/SRHB.pdf> (2023). Accessed 29 February 2024
4. Andøya Space: DLR MORABA SOAR Campaign from @Andøya Space | Day 1. <https://www.youtube.com/watch?v=3hKwi1GfSko> (2023). Accessed 8 March 2024